

Image Segmentation and Center Positioning Method for Roughcast Wheel Hubs under Complex Background

Jia-Lin Cui and Bin Lian

School of Information Science and Engineering
NingboTech University
Ningbo 315100, P.R. China
cuijl_jx@163.com

Guang-Yu Kang

School of Control and Mechanical Engineering
Tianjin Chengjian University
Tianjin 300222, P.R. China
kgycat250318@sina.com

Zhe-Ming Lu*

School of Aeronautics and Astronautics
Zhejiang University
Hangzhou 310027, P.R. China
*Correponding Author: zheminglu@zju.edu.cn

Yeh-Cheng Chen

Department of Computer Science
University of California
Davis, USA
ycch@ucdavis.edu

Received February 2020; Revised October 2020

ABSTRACT. *The precise positioning of the borehole during the automated finishing process of the automotive wheel hub is an urgent problem to be solved. Conventional positioning is done by mechanical fixtures, but the burrs of the hub can cause misalignment. The vision-based center positioning algorithm is often limited by complex background environment. This paper proposes a precise positioning method in complex background environment. This method uses superpixel algorithm to segment the image into several clustering regions and then calculate the gradient energy of each cluster, and the edge image data of the wheel hub is obtained. On this basis, the key data of the hub side is extracted, and the center and radius of the hub are accurately fitted. Finally, the effectiveness of the proposed method is verified by experimental comparison.*

Keywords: Wheel hub, Center positioning, Image segmentation, Machine vision, Superpixel.

1. **Introduction.** The wheel hub is an important part of the automobile. In the manufacturing process, after multiple processes, the hub center drilling positioning mechanism currently generally adopts mechanical fixture positioning, and there is no automatic identification and positioning function. Due to the influence of the irregular burrs of the

blank hub, the positioning of the mechanical clamp often leads to differences in positioning accuracy and a certain product defect rate. In this paper, the positioning method of machine vision is used to accurately locate the center point of the hub by taking advantage of the captured front image of the hub. The difficulty in identifying the center point is that the hub burr also affects the accuracy of the calculation. In addition, the complex background environment interferes with the segmentation of the hub image. There are a lot of researches and applications at home and abroad on the research on the method of center positioning.

The Hough transform (HT) was proposed by Paul Hough, and the researchers have continuously improved it and applied it extensively to the detection of circles [1-4]. The HT method has universally applicable advantages for finding circles in various images, and thus has been widely adopted so far, but the calculation amount of the three-dimensional space used by HT is huge, and it is often difficult to satisfy online real-time detection. In terms of hub center point detection, Chen and Lin [5] proposed a high-precision detection method for wheel center based on stereo vision. The method of measuring the wheel gauge, wheel difference and wheel static radius of three models proved the effectiveness of wheel center detection of the proposed method. In the literature [6], considering the positioning error caused by the large amount of interference in the bottle mouth image during the quality inspection of beer bottles, a bottle mouth positioning algorithm for multiple random circle detection and round fitting evaluation was proposed. In this method, threshold segmentation, the central method and the radial scanning method were used, and a circle is randomly determined by using 3 randomly sampled points, which has some reference significance to this paper.

In the complex background, the segmentation and contour extraction of the hub image is a difficult point. Image segmentation is a process of dividing the image space into a certain number of regions according to the characteristics of grayscale, frequency, texture, etc. Currently, the commonly used segmentation algorithms are threshold method [7], region growing method [8], watershed segmentation method [9], Mean Shift algorithm [10] and edge detection method [11]. In 2003, Wang et al. proposed a superpixel method [12], which refers to a local, consistent, small area in the image that maintains the local structural features of a certain image. Superpixels have been widely used in the field of image segmentation [13]. The existing superpixel methods are roughly divided into two categories: graph theory based algorithms and gradient rise based algorithms [14]. And the literature [15] selects six kinds of superpixel algorithms, such as SL, Turbopixel, GCa, SLIC, ERS, and SEEDS, to carry out quantitative analysis and comparison. In comparison, SLIC and SEEDS have better performance in terms of superpixel tightness and edge fit. Directly adopting the segmentation algorithm as described above, it is impossible to segment the hub in the complex background. There are also other schemes based on deep learning and feature extraction[16-21]. In this paper, SLIC is used as an important preprocessing method for hub segmentation, and the energy gradient of each superpixel is calculated. Based on this, a wheel splitting based on super-pixel energy spectrum is proposed, which can effectively segment the hub and finally fit through the key point data to obtain satisfactory segmentation and center positioning.

2. Proposed Wheel Hub Segmentation Based on Superpixel Energy Spectrum.

In the hub production workshop, due to the color closeness between the metal roller of the conveyor transmission line and the hub, and the interference of external ambient light, the segmentation of the hub color and the background color of the conveyor line is difficult. At the same time, due to the flash of the hub edge caused by the wear of the abrasive tool during the casting process of the hub, resulting in mechanical fixture

positioning deviation. Aiming at the above problems, combined with the characteristics of the blank hub itself, this paper proposes a new positioning algorithm for the center positioning of the blank hub. The algorithm mainly includes two major steps: wheel image segmentation and wheel fine positioning. For the image segmentation of the hub in complex background, this paper adopts the superpixel method to cluster the whole image, and calculates the gradient energy map based on the clustering segmentation, which can further expand the saliency of the hub circumference. The steps for wheel hub segmentation based on superpixel segmentation are as follows:

Step 1: At intervals of M grid nodes, initial K cluster centers $V_k = (C_k, S_k)$, $k = 1, 2, \dots, K$, uniformly on the image, where $C_k = (l_k, a_k, b_k)$ and $S_k = (x_k, y_k)$ denote the three-dimensional color vector in the CIE-LAB color space and two-dimensional spatial coordinates of the k -th cluster center.

Step 2: Select 3×3 pixels with minimum gradient in the neighborhood as the new cluster centers, and distribute pixels in cluster centers based on distance measure, and then give the index of the nearest cluster center to all pixel points. Here, the normalized distance based on color and spatial characteristics is defined as

$$D(i, j) = \sqrt{\left(\frac{\|C_i - C_j\|}{N_c}\right)^2 + \left(\frac{\|S_i - S_j\|}{N_s}\right)^2} \quad (1)$$

where the vector C_k means the k -th three-dimensional color vector in the CIE-LAB color space, the vector S_k represents the k -th two-dimensional spatial coordinates, $j = 1, 2, \dots, K$ is the index of cluster center, and the subscript i is the pixel index in the $2M \times 2M$ sized neighborhood of the corresponding cluster center j . Here, $M = \sqrt{\frac{N}{K}}$, N is the total number of pixels in the image, and N_c, N_s are the normalization constants of color distance and space distance respectively.

Step 3: After the initialization of clusters, the K cluster centers φ_j , $j = 1, 2, \dots, K$ iteratively update based on the colors and the mean spatial characteristics of all the pixels in the corresponding image block G_j ,

$$\varphi_j = \frac{1}{N_j} \sum_{j \in G_j} V_j \quad (2)$$

where N_j is the number of pixels in the image block G_j .

Step 4: Repeat Steps 2 and 3, recalculate the cluster centers, re-clustering and repeat the iterative operation and calculate the distance E between two clustering centers until the distance E is less than the threshold value. In the end, the adjacent merging strategy is adopted to eliminate the isolated small-sized superpixels, which can ensure the final result to have a good degree of compactness.

Step 5: Calculate the gradient energy matrix based on the super-pixel as follows:

First, construct the local gradient function of superpixel φ_k as

$$G_{-\varphi}(k) = \frac{1}{A_k} \sum_{m=1}^{\alpha_k} \sum_{n=1}^{\beta_k} \sqrt{\frac{(B(m, n) - B(m+1, n))^2 + (B(m, n) - B(m, n+1))^2}{2}} \quad (3)$$

$B(m, n)$ is the gray value at the center (m, n) , α_k is the horizontal coordinate upper limit of the super-pixel φ_k , β_k is the vertical coordinate upper limit of the super-pixel φ_k , and A_k is the area of the super-pixel.

The gradient can reflect the edge information of the image, the bigger the gradient value is, the more obvious the characteristics are. A higher gradient value means richer edge information.

Relying solely on the gradient can easily cause the loss of the high frequency component of image information. Furthermore, construct the local energy function of the superpixel region φ_k as

$$E_{-\varphi}(k) = \sum_{m=1}^{\alpha_k} \sum_{n=1}^{\beta_k} (B(m, n))^2 \quad (4)$$

The energy function reflects the richness of image information, which ignores the characteristics of image information and contains a large number of information of the fuzzy regions. Also construct a local variance function as

$$C_{-\varphi}(k) = \sum_{m=1}^{\alpha_k} \sum_{n=1}^{\beta_k} (B(m, n) - \bar{B}_k)^2 \quad (5)$$

where \bar{B}_k is the average gray value of the super-pixel. The variance can reflect the change degree and the dispersion degree of the pixels in the region. And finally, we integrate the three conditions above and construct an integrated gradient function of the energy variance is

$$GEC(k) = \lambda \cdot G_{-\varphi}(k) + \delta \cdot E_{-\varphi}(k) + \xi \cdot C_{-\varphi}(k) \quad (6)$$

where λ is the gradient coefficient, δ is the energy coefficient, and ξ is the variance coefficient.

Step 6: According to the gradient energy matrix obtained from Step five, combined with the superpixel region space, the gradient energy map of the image can be calculated, and the wheel edge information can be further enhanced. The general outline of the hub is segmented by scanning the gradient energy map.

Step 7: According to the outline obtained from above step, the reference center (x', y') of the hub and the radius' reference value R' can be obtained. Hough transform is carried out with $r \in (R' - 10, R')$ as the scanning range, then calculate the fitting value of the segmentation center (x'_0, y'_0) and radius r' , and preserving the pixel points which have a larger ranging gradient to avoid the loss of the information of the support pixels.

3. Proposed Exact Circle Fitting Method. The algorithm mainly includes radius scanning, straight line fitting, radius compensation, burring point removal, least squares fitting and so on. According to the boundary of the image after the hub is segmented, the center and radius are preliminarily calculated. Then, based on the center and radius, 360 edge points are scanned in the radial direction, and the distance from each edge point to the preliminary center point is calculated, and then the mean method is used. The scan data is compensated, and from the compensated radius data the longer distance point and the shorter point are removed, and finally the least squares method is used to fit the center and the radius. The steps are as follows:

Step 1: Obtain the radial distance of edge points by radial scanning.

Set the preliminary center point (x_0, y_0) as the reference, set the radial scanning range within the ring ranging from $r - 20$ to $r + 20$. Repeat the radial scanning for a total of W times, and the radial scanning step angle is $360/W$, here W equals to 360. Set alf as the scanning angle, where $alf \in [1, 360]$. The scanning range is represented by len , where $len \in [r - 20, r + 20]$. Thus, The coordinates of the scanned edge points are

$$x_i = \text{round}(len(i) * \cos(alf * \pi/180) + x_0) \quad (7)$$

$$y_i = \text{round}(len(i) * \sin(alf * \pi/180) + y_0) \quad (8)$$

The binarized image data is scanned radially from the distance of $r + 20$ to the center of the circle. When a white point is encountered, it is considered as an edge point, and the coordinates of the point are recorded. Comparing with the two wheels which are smooth

and burr, scanning the distance edge points between the initial center (x_0, y_0) and the edge points.

Step 2: Data preprocessing of edge points.

The ideal edge corresponds to the exact center of the circle, and the edge point scanned data should be a horizontal line. However, the actual data may be affected by two aspects: on the one hand, the raw edges cause the data to be unsmooth, on the other hand, if the initial center (x_0, y_0) is located with deviation, the overall data will be affected.

In this paper, the mean value method is used to adaptively offset the edge data points. The mean smoothing interval is P points. The deviation compensation formula is as follows:

$$rr(i) = rr(i) - \left[\frac{1}{P} \sum_{n=i}^{i+P} rr(n) - \frac{1}{W} \sum_{j=1}^W rr(j) \right] \quad i \in [1, W] \quad (9)$$

Where $rr(i)$ is the distance from the edge point to the center of the circle, P is the number of smooth points, and W is the total number of edge points. The corresponding coordinates of the edge point is recorded as $(x_i, y_i), i \in [1, W]$.

Sort the data after repair, and eliminate the minimum 10 points, and take $P - 10$ points of data between 11 and P from small to large. Use this set of data as input data for the final circle fitting.

Step 3: Least squares fitting.

If the above data preprocessing is not done, the circle is directly fitted by the least squares method, and the fitting result will receive the influence of the glitch, which makes it difficult to accurately locate the center of the circle. The least squares method is a mathematical optimization technique that finds the best matching function for a set of data by minimizing the sum of the squares of the errors. Now to fit the circular curve, let the circular curve equation be:

$$r^2 = (x - x_0)^2 + (y - y_0)^2 \quad (10)$$

After expansion, you can get another form of the circular curve:

$$x^2 + y^2 + ax + by + c = 0 \quad (11)$$

In order to find the optimal circle fitted by the least squares method, the following summed variance function is introduced:

$$U(a, b, c) = \sum_{i=1}^W \varepsilon_i^2 = \sum_{i=1}^W (x_i^2 + y_i^2 + ax_i + by_i + c) \quad (12)$$

To get the minimum $U(a, b, c)$, we can set the partial derivative of a, b, c for this function to 0:

$$\frac{\partial U(a, b, c)}{\partial a} = \frac{\partial U(a, b, c)}{\partial b} = \frac{\partial U(a, b, c)}{\partial c} = 0 \quad (13)$$

From the above equation, the coefficients a, b and c can be obtained, and then the center coordinates (x_0, y_0) and radius r can be obtained.

4. Analysis of the Results of Circle Fitting.

4.1. Test Environment. In this paper, the hardware environment of the positioning system includes an equipment box (blue), an industrial HD CCD camera and a Mega pixel camera (on the top of the blue box body), an Advantech industrial PC (with a panel in the middle), a machine vision ring light source, transmission and positioning mechanisms, and a PLC control system and other ancillary equipments, On the left side

of Fig. 1, there are the working interface and the identification system box, and on the right side, it shows the wheel hub is lining up into the drilling machine.



FIGURE 1. Recognition and location system debugging site.

4.2. Wheel Hub Segmentation. An example original picture of the hub captured on the spot is shown in Fig. 2(a). According to the first step of the whole algorithm, the superpixel segmentation operation is performed on the original picture, and the initial number of clusters is 400. After the SLIC superpixel segmentation, the grid diagram of the clustering region is shown in Fig. 2 (b).

After the superpixel segmentation, the gradient energy variance $GEC(k)$ is used to calculate the comprehensive energy value of gradient variance for each pixel. And the gradient energy diagram calculated by combining the original super-pixel point is shown in Fig. 2(c), it can be seen from the figure that the peripheral edge information of the contour is greatly enhanced. Fig. 2(d) shows the coarse segmentation. Finally, after the Hough Transform, combined with the wheel hub edge information, the wheel hub image can be divided more accurately, as is shown in Fig. 2(e). After the wheel hub image segmentation, the next step is the implementation of the accurate wheel hub circle fitting algorithm. As is shown in Fig. 3, the interference of the number of the burrs' on the wheel hub edge point is very obvious, which will affect the accurate positioning of the wheel hub center and the measurement of image's radius. In Fig. 3(a), the edge is smooth, the burr is less and the scanned data is smooth. However, in Fig. 3(b), the data fluctuation is obvious due to much burr.

Because of the burr bias on one side, a preliminary locating deviation happens and the value of the edge will be volatile, which impact the follow-up data selection. Fig. 4 shows the scanned data waveform when the horizontal or vertical coordinates have different deviations is respectively 1 pixel, 5 pixels and 10 pixels. The red curve is the scanning value of time, the blue curve shows the situation after using the Mean Method. After the compensation under different deviation situation the effect without deviation can be reduced.

Now, the comparison among the Hough transform method, the radial scanning average method, the least squares method, the centroid method and our method is shown as the following subsection.

4.3. Positioning Accuracy Test. In order to verify the effectiveness and superiority of our method, 8 images with larger interference were selected to detect the circle among about 300 pictures extracted from the identification system. We compare the center and the radius located by different methods with the real value which is the number of the

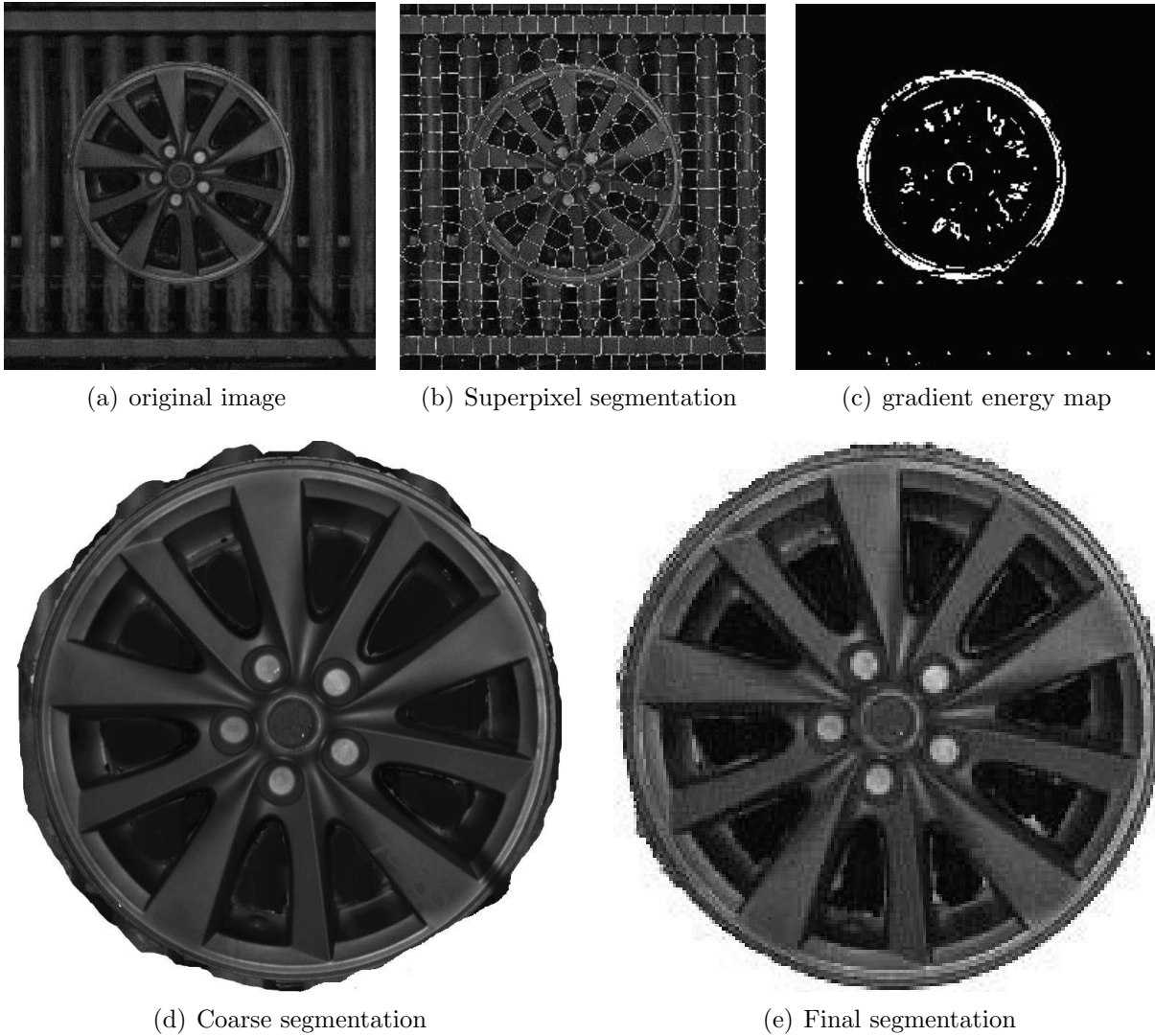
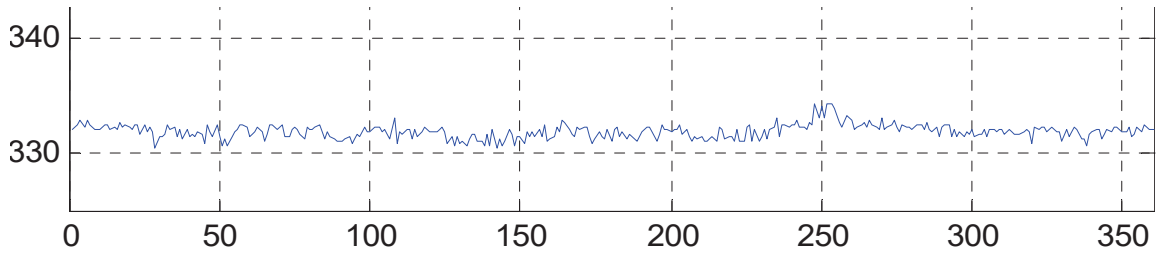


FIGURE 2. Image segmentation results.

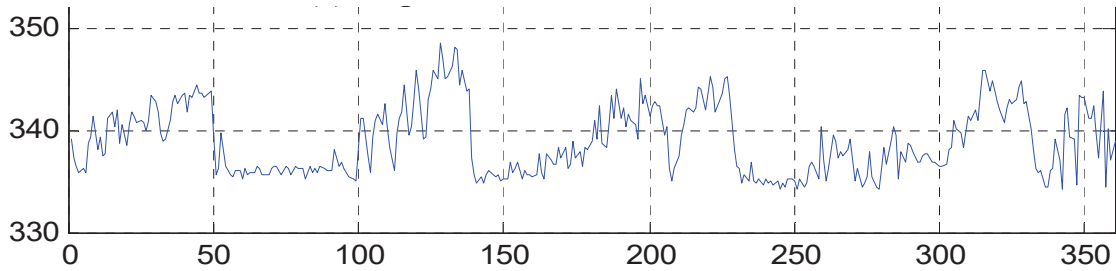
pixels in the picture after removing the burrs. Several commonly used circle detection algorithms are the Hough transform method, the least squares method, the radius scanning average method, the centroid method and the method in this paper. The least squares method is a method that uses edge points without preprocessing.

The running efficiency of these algorithms is also compared. The time consumption of our algorithm is equivalent to the least squares method. And our method is much faster than the Hough transform method and the centroid method, which can meet the requirements of real time. The recognition of the algorithm in this paper is with a higher positioning accuracy and its measured deviation is the least. The comparison results are shown in Fig. 5, where ΔR is the radius deviation, Δx is the horizontal coordinate deviation of the center, Δy is the vertical coordinate deviation of the center. The pink line in Fig. 5 shows the result of this paper, most of the deviations are zeros, and deviations within ± 2 are with a small number, which means the accuracy of our method is significantly better than several existing circle location algorithms.

5. Conclusions. A wheel segmentation based on superpixel energy spectrum is proposed in this paper. Experiments show that the combination of superpixel segmentation and



(a) Edge data from smooth wheel hub



(b) Edge data from wheel hub with serious burr

FIGURE 3. Edge data from different wheel hub segmentation image.

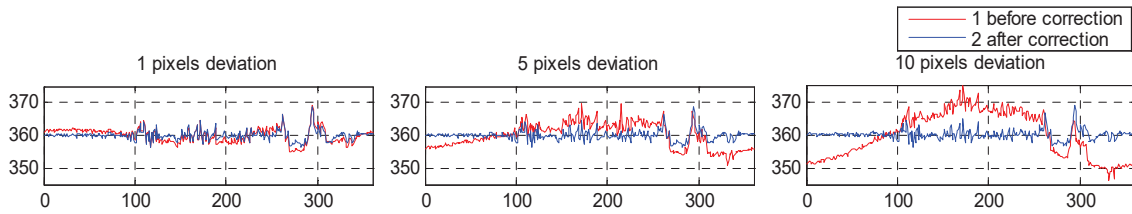


FIGURE 4. The comparison of edge data under the preliminary circle center with different deviation and the data after compensation.

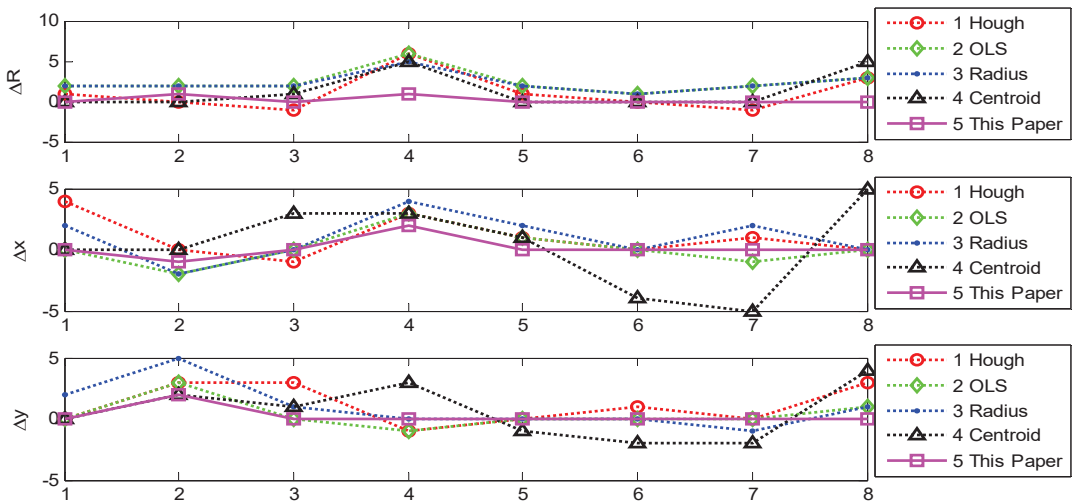


FIGURE 5. Comparisons of radius and center positioning error among five algorithms.

gradient energy can greatly improve the saliency of the hub edge, and it is effective for the extraction and segmentation of the hub contour in the complex background. Secondly, our method can accurately locate the center, and the key point data of the hub is used instead of all. The edge data is compensated by the mean method, which improves the anti-interference and the robustness of the center-fitting. Our method also has a higher computing efficiency. Compared with the Hough transform method, the centroid method, the least squares method and the radius scanning method, our method can locate the center of the hub more effectively.

Acknowledgment. This work is partially supported by the financial support from the Zhejiang Provincial Natural Science Foundation of China under grant No. LY16F010019, No. LY17F020019 and No.19F030005, Ningbo Sci. & Tech. innovation team plan project (2014B82015) and the National Natural Science Foundation of China under grant No.61633019 and No.61972350. This research work is also partially supported by Ningbo Science and technology innovation 2025 major project(2019B10116), National Key R&D Program of China (No.2018YFB1702200).

REFERENCES

- [1] R. Chan, New parallel Hough trans for for circles, *IEEE Proceedings E-Computers and Digital Techniques*, vol. 138, no. 5, pp.335–334, 1991.
- [2] E. Cuevas, F. Wario, V. Osuna-Enciso, et al, Fast algorithm for multiple-circle detection on images using learning automata, *IET Image Processing*, vol. 6, no. 8, pp. 1124–1135, 2012.
- [3] H. Maitre, Contribution to the prediction of performances of the hough transform, *IEEE Transactions on Pattern Analysis and Machine Intelligence*, vol. 8, no. 5, pp. 669–674, 1986.
- [4] L. Xia, C. Cai, C. P. Zhou, et al. New fast algorithm of Hough transform detection of circles, *Application Research of Computers*, vol. 24, no. 10, pp. 197–200, 2007.
- [5] X. Chen, G. Lin, Wheel center detection based on stereo vision, *Journal of Southeast University(English Edition)*, vol. 29, no.2, pp. 175–181, 2013.
- [6] X. Zhou, Y. Wang, K. Li, et al. New bottle mouth positioning method based on multiple randomized circle detection and fitting degree evaluation, *Chinese Journal of Scientific*, vol. 36, no. 9, pp. 2021–2029, 2015.
- [7] P. K. Sahoo, S. Soltani, A. K. C. Wong, et al., Survey of thresholding techniques, *Computer Vision, Graphics, and Image Processing*, vol. 31, no. 2, pp. 233–260, 1988.
- [8] S. Pohlman, K. A. Powell, N. A. Obuchowski, et al, Quantitative classification of breast tumors in digitized mammograms, *Medical Physics*, vol. 23, no. 8, pp. 1337–1345, 1996.
- [9] L. Vincent, and P. Soille, Watersheds in digital spaces: an efficient algorithm based on immersion simulations, *IEEE Transactions on Pattern Analysis and Machine Intelligence*, vol. 13, no. 6, pp. 584–598, 1991.
- [10] Y. Z. Cheng, Mean shift, mode seeking, and clustering, *Pattern Analysis and Machine Intelligence*, vol. 17, no. 8, pp. 790–799, 1995.
- [11] R. C. Gonzalez, and R. E. Woods, *Digital Image Processing*, 2nd ed, Beijing: Publishing House of Electronics Industry, pp. 463–473, 2003.
- [12] C. Y. Wang, J. Z. Chen, and W. Li, Superpixel segmentation algorithms review, *Journal of Application Research of Computers*, vol. 31, no. 1, pp. 6–12, 2014.
- [13] X. Ren, and J. Malik, Learning a classification model for segmentation, *Proceedings of the IEEE International Conference on Computer Vision*, Washington DC, USA: IEEE, pp. 10–17, 2003.
- [14] R. Achanta, A. Shaji, K. Smith, et al., SLIC superpixels compared to state-of-the-art superpixel methods, *IEEE Transactions on Pattern Analysis and Machine Intelligence*, vol. 34, no. 11, pp. 2274–2282, 2012.
- [15] X. Y. Song, L. L. Zhou, Z. G. Li, J. Chen, L. Zeng, and B. Yan, Review on superpixel methods in image segmentation, *Journal of Image and Graphics*, vol. 20, no. 5, pp. 0599–0608, 2015.
- [16] K. K. Tseng, R. Zhang, C. M. Chen, M. M. Hassan, DNetUnet: a semi-supervised CNN of medical image segmentation for super-computing AI service, *The Journal of Supercomputing*, pp. 1–22, 2020.

- [17] E. K. Wang, C. M. Chen, M. M. Hassan, and A. Almogren, A deep learning based medical image segmentation technique in Internet-of-Medical-Things domain, *Future Generation Computer Systems*, vol. 108, pp. 135–144, 2020.
- [18] E. K. Wang, C. M. Chen, F. Wang, M. K. Khan, and S Kumari, Joint-learning segmentation in Internet of drones (IoD)-based monitor systems, *Computer Communications*, vol. 152, no. 2, pp. 54–62, 2020.
- [19] F. Zhang, T.-Y. Wu, J.-S. Pan, G. Ding, and Z. Li, Human motion recognition based on SVM in VR art media interaction environment, *Human-centric Computing and Information Sciences*, vol. 9, 40, 2019.
- [20] E. K. Wang, X. Zhang, F. Wang, T.-Y. Wu, C.-M. Chen, Multilayer dense attention model for image caption, *IEEE Access*, vol.7, pp.66358-66268, 2019.
- [21] F. Zhang, T.-Y. Wu, and G. Zheng, Video salient region detection model based on wavelet transform and feature comparison, *EURASIP Journal on Image and Video Processing*, vol. 2019, no.1, 58, 2019.